NASA TECHNICAL NOTE

NASA TN D-6370

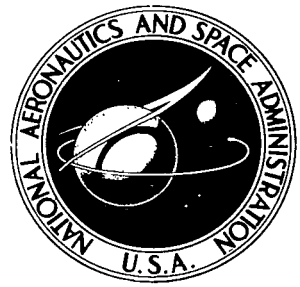

CORRELATION OF SECONDARY SONIC AND SUPERSONIC GASEOUS JET PENETRATION INTO SUPERSONIC CROSSFLOWS

by Frederick P. Povinelli and Louis A. Povinelli

Lewis Research Center
Cleveland, Ohio 44135

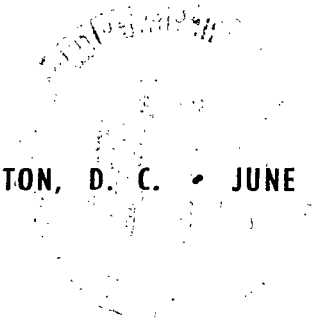

NATIONAL AERONAUTICS AND SPACE ADMINISTRATION • WASHINGTON, D. C. • JUNE 1971

1. Report No. NASA TN D-6370	2. Government Accession No.	3. Recipient's Catalog No.
4. Title and Subtitle CORRELATION OF SECONDARY SONIC AND SUPERSONIC GASEOUS JET PENETRATION INTO SUPERSONIC CROSSFLOWS		5. Report Date June 1971 6. Performing Organization Code
7. Author(s) Frederick P. Povinelli and Louis A. Povinelli		8. Performing Organization Report No. E-6128
9. Performing Organization Name and Address Lewis Research Center National Aeronautics and Space Administration Cleveland, Ohio 44135		10. Work Unit No. 722-03 11. Contract or Grant No.
12. Sponsoring Agency Name and Address National Aeronautics and Space Administration Washington, D. C. 20546		13. Type of Report and Period Covered Technical Note 14. Sponsoring Agency Code

15. Supplementary Notes

16. Abstract

Helium was injected from a flat plate normal to Mach 2 and Mach 3 airstreams at various injection Mach numbers ranging from sonic to Mach 4. Concentration measurements were taken downstream of the secondary injection location for a range of injection and tunnel total pressures. Supersonic injection resulted in as much as a 30 percent increase in penetration over that obtained for equal mass flow sonic injection. An equation based on jet Mach number, pressure ratio between the jet and free stream, and downstream distance was obtained which correlated the data to within ±10 percent. Penetration data from four other studies were compared with the present data and were correlated when the boundary layer momentum loss was considered.

17. Key Words (Suggested by Author(s)) Jet penetration Sonic injection Supersonic injection Supersonic flow Concentration Correlation Wind tunnel Flat plate	18. Distribution Statement Unclassified - unlimited	
19. Security Classif. (of this report) Unclassified	20. Security Classif. (of this page) Unclassified	21. No. of Pages 21 / 22. Price* $3.00

*For sale by the National Technical Information Service, Springfield, Virginia 22151

CORRELATION OF SECONDARY SONIC AND SUPERSONIC GASEOUS JET PENETRATION INTO SUPERSONIC CROSSFLOWS

by Frederick P. Povinelli and Louis A. Povinelli

Lewis Research Center

SUMMARY

The effect of injection Mach number on the penetration of secondary jet injection into a supersonic primary stream was determined. Helium was injected from a flat plate normal to Mach 2 and Mach 3 airstreams at eight injection Mach numbers varying from 1 to 4. Concentration measurements were taken on the jet centerplane and the penetration defined as the height at which the helium concentration dropped to 0.5 percent. Injectant and tunnel total pressures were also varied. Jet penetration was found to increase with jet Mach number, a maximum increase of about 30 percent being obtained when comparing Mach 4 to sonic injection for equal mass flows. Jet penetration also increased with the ratio of jet total to effective back pressure and with downstream distance from the injection location. An equation based on these parameters correlated the penetration data to within ±10 percent.

When penetration data from four other studies were compared with the present data, an additional term accounting for boundary layer momentum loss was used to correlate all of the data. When the data were separated into near and far field regions, improvement in the correlation was obtained in the far field.

INTRODUCTION

The injection of secondary jets into a supersonic primary airstream has been studied extensively in the last half decade, quite often for application to supersonic combustion ramjet engines. In such an engine concept, the airflow through the combustion chamber is supersonic rather than subsonic as in a conventional ramjet engine. The high momentum of the supersonic airstream causes the injected fuel to be turned rapidly downstream, limiting mixing and combustion efficiency. Thus injection schemes which help alleviate the fuel distribution problem are of interest.

The most extensively studied aspect of fuel injection has been the penetration of normal sonic jets into a supersonic airstream (refs. 1 to 7). Some attention (refs. 8 to 11) has been given to normal supersonic injection; the results indicate that more penetration can be obtained with this method of injection. Existing data, however, are available over only a limited Mach number range and the studies vary in their definition of penetration making comparisons and corroborative conclusions difficult. The purpose of this present study was to determine the effect of injection Mach number on jet penetration over a wide range of jet Mach numbers and pressures with variations in free stream Mach number and pressure.

Helium was injected at various pressures from a flat plate mounted in a supersonic wind tunnel. Injection Mach number was varied from sonic to Mach 4, and free stream Mach numbers of 2 and 3 were employed. Concentration measurements downstream of the injection point were used to characterize the jet penetration. The data were correlated with an expression containing a jet to free stream pressure ratio, jet Mach number, and downstream distance. Comparisons were made with sonic and supersonic injection data in the literature. Portions of this work were previously reported in reference 12.

SYMBOLS

a,b,c,d,C	constants in correlation equations
d_e	injector nozzle exit diameter
d^*	injector nozzle throat diameter
ℓ	distance from leading edge of flat plate to injection nozzle centerline
M	Mach number
P_{eb}	effective back pressure (two-thirds of total pressure behind a normal shock in free stream)
P_o	total pressure
Re_L	free stream Reynolds number at injection location
v	velocity
x	downstream distance from nozzle centerline
y	vertical coordinate
y'	penetration (0.5 mole percent concentration point) measured normal to plate surface
γ	specific heat ratio

δ	boundary layer velocity thickness
θ	boundary layer momentum thickness
ρ	density

Subscripts:

a	free stream
j	jet

APPARATUS AND PROCEDURE

Model and Tunnel

A flat-plate model was installed to span the 25.4- by 9.75-centimeter test section of a supersonic wind tunnel as shown in figure 1. A 0.318-centimeter-diameter hole was drilled into the model to supply helium from a cylinder bank to the injection nozzles. Various injector inserts were flush mounted by threading them into the top surface of the flat plate as shown in figure 2 for the sonic nozzle. A spanner wrench was used to tighten the inserts down on an O-ring for a pressure tight seal. The spanner wrench notches were filled and sanded after each nozzle installation. The injector hole was located on the plate and tunnel centerlines 5.82 centimeters from the leading edge of the model and

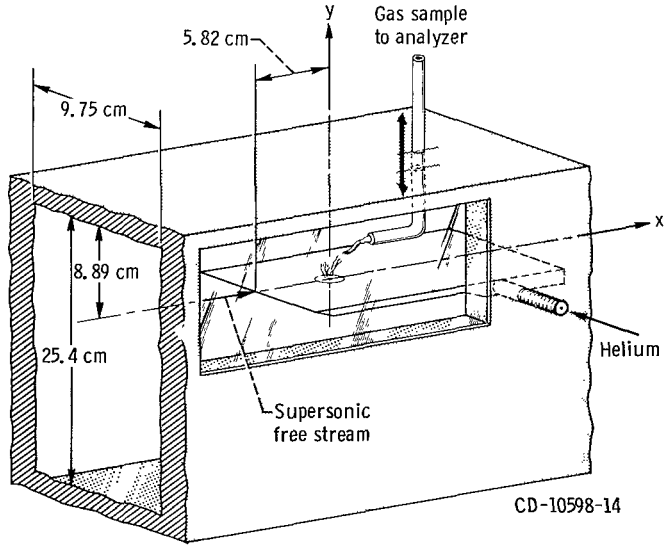

Figure 1. - Flat-plate model installed in supersonic funnel.

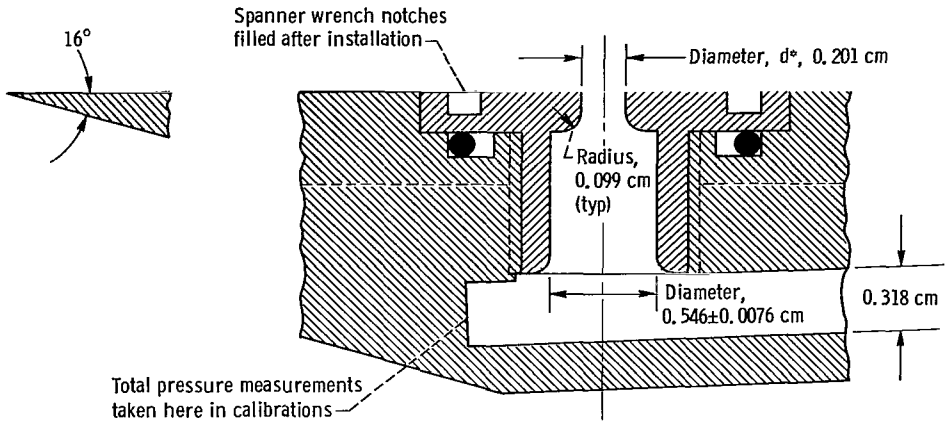

Figure 2. - Cross-sectional view of sonic nozzle installed in flat plate.

8.89 centimeters from the top wall of the tunnel. All nozzles had the same external dimensions and internal radii and had throat diameters of 0.203±0.002 centimeter.

The exit Mach numbers for the supersonic nozzle inserts were determined with helium injected into still air. Hypodermic tubes of 0.051-centimeter outside diameter were used to measure the Pitot pressure at the nozzle exit and the total pressure in the model passage. The exit Mach number was obtained from the Pitot to total pressure ratio and compressible flow tables for $\gamma = 1.667$. For the four supersonic nozzles for which the bulk of the penetration data were taken, Mach number calibration curves are shown in figure 3 as a function of injection total pressure for three ambient back pressures. The total expansion angle for these nozzles was 17°. (Nozzle cross sections and dimensions are shown as insets.) The jet Mach numbers M_j determined from the pressure measurements were 2.37, 2.67, 3.52, and 3.99 and differed from those calculated from the measured throat and exit diameters by less than 10 percent. A limited amount of penetration data was taken for three other nozzles calibrated to have exit Mach numbers of 1.69, 2.75, and 2.91 with total expansion angles of 17°, 11°, and 8°, respectively.

As the ambient pressure was lowered (fig. 3), a total pressure was reached at which the nozzle flow separated. When helium was injected into the supersonic crossflow rather than into still air as in the nozzle calibration tests, it was no longer obvious what back pressure the jet experienced due to the complex pressure and shock patterns caused by the interaction of the jet with the main flow stream. If the free stream static pressure could be used to define the back pressure, then all nozzles would flow full for the total pressures used to obtain the penetration data. Another back pressure which could possibly control nozzle flow was suggested in reference 6 as 80 percent of the static pressure behind a normal shock in the free stream. For tunnel conditions of this study, this second definition of back pressure was 43 kilonewtons per square meter or less. If this is

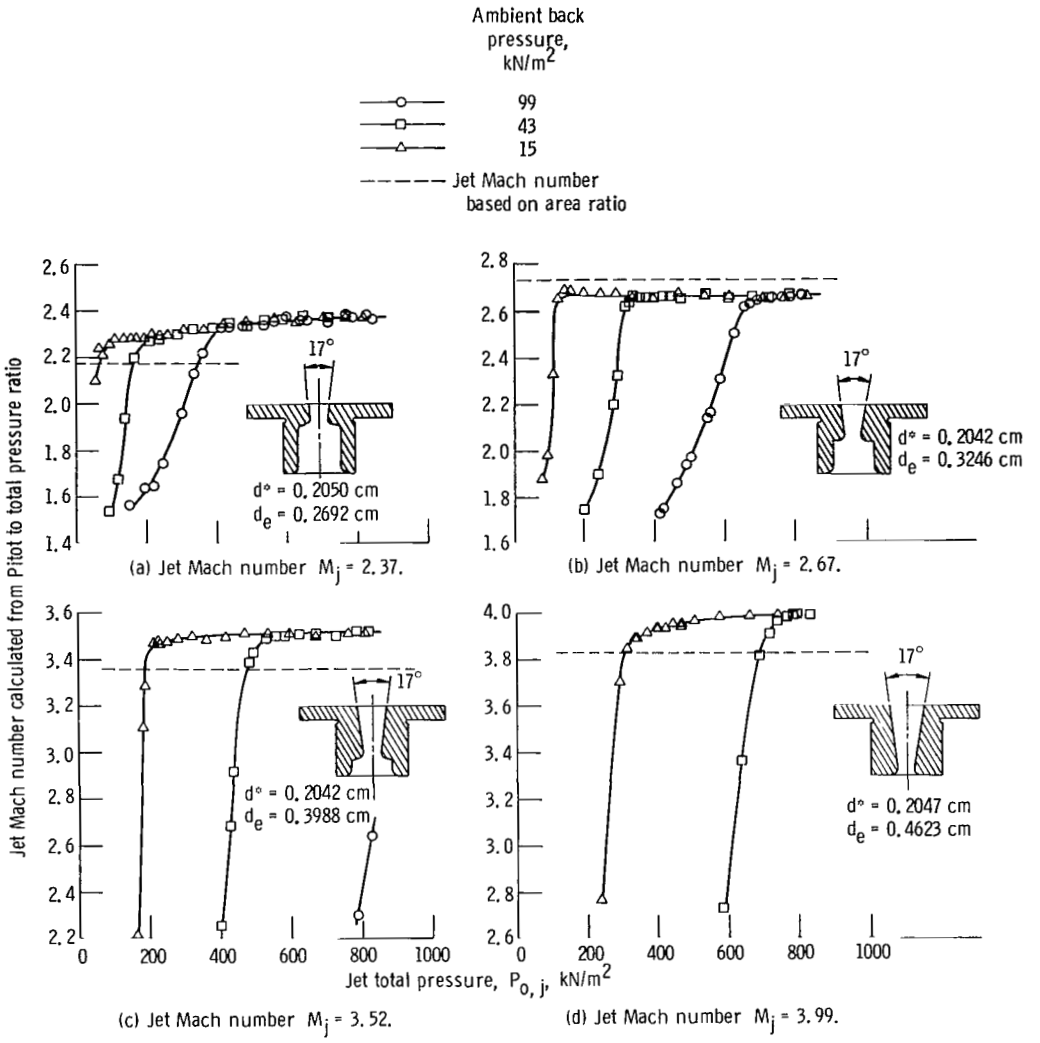

Figure 3. - Calibration of conical supersonic nozzles.

the appropriate back pressure to determine if nozzle flow separation occurred, two of the total pressures used at $M_j = 3.99$ (namely, 517 and 690 kN/m^2) could result in separated nozzle flow. The penetration data at these conditions were inspected with this possibility in mind.

The supersonic wind tunnel was equipped with removable nozzle blocks allowing test conditions at free stream Mach numbers of 2 and 3. Tunnel total pressure was varied from 58.7 to 93.4 kilonewtons per square meter at a constant total temperature of 348 K. The Reynolds number at the injection location Re_L ranged from 2.44×10^5 to 5.35×10^5.

TABLE I. - TEST CONDITIONS AND RESULTS

Jet Mach number, M_j	Free stream Mach number, M_a	Jet total pressure, $P_{o,j}$, kN/m^2	Jet to free stream total pressure ratio, $\frac{P_{o,j}}{P_{o,a}}$	Nondimensional downstream distance, $\frac{x}{d^*}$	Penetration, $\frac{y'}{d^*}$
1.0	2.0	331	3.55	4.1	4.68
		517	5.54		5.81
		690	7.39		6.76
		897	9.60		7.55
		517	5.54	10.1	7.53
		690	7.39	10.1	8.76
		517	5.54	16.7	7.81
		690	7.39	16.7	9.15
		897	9.60	16.7	10.48
		517	5.54	17.2	7.95
		690	7.39		9.16
		517	6.80		8.55
		690	9.07		[a]10.03
		517	8.81		[a]9.56
		690	11.75		[a]11.23
		517	5.54	17.8	8.20
		690	7.39		9.36
		517	6.80		8.93
		690	9.07		10.28
		517	8.81		10.03
		690	11.75		11.60
	3.0	517	5.54	17.2	12.01
		517	6.80		13.23
		690	7.39		13.69
		690	9.07		14.86
		517	5.54	4.0	8.53
		690	7.39	4.0	9.59
1.69	2.0	517	5.54	17.8	8.76
		690	7.39		9.93
		690	9.07		11.00
		690	11.75		12.65
2.37	2.0	386	4.14	4.1	5.41
		517	5.54		6.34
		890	7.39		7.40
		897	9.60		8.40
		517	5.54		8.65
		690	7.39	10.1	10.20
		517	5.54	16.7	8.93
		690	7.39	16.7	10.75
		897	9.60	16.7	12.38
2.67	2.0	483	5.17	4.1	6.01
		517	5.54		6.28
		690	7.39		7.41
		897	9.60		8.36
		517	5.54	17.8	9.49
		690	7.39	17.8	11.34
		517	6.80	17.8	10.78
	3.0	517	5.54	16.7	13.84
		690	7.39	16.7	16.00
		690	9.07	16.7	17.25
2.75	2.0	517	5.54	17.8	9.48
		690	7.39		11.26
		517	6.80		10.89
		690	9.07		12.83
	3.0	517	5.54	16.7	14.01
		690	7.39	16.7	16.09
		690	9.07	16.7	17.38
2.91	2.0	517	5.54	17.8	10.00
		690	7.39		11.83
		517	6.80		11.73
		690	9.07		13.84
3.52	2.0	517	5.54	4.1	6.36
		690	7.39	4.1	7.45
		897	9.60	4.1	8.44
		517	5.54	16.7	9.13
		690	7.39	16.7	11.08
		897	9.60	16.7	12.88
3.99	2.0	517	5.54	4.1	6.49
		690	7.39	4.1	7.60
		897	9.60	4.1	8.55
		517	5.54	10.1	8.98
		690	7.39	10.1	10.64
		517	5.54	16.7	9.58
		690	7.39	16.7	11.38
		897	9.60	16.7	13.13
		517	5.54	17.2	9.85
		690	7.39		11.63
		517	6.80		10.94
		690	9.07		[a]13.05
		517	8.81		[a]12.65
		690	11.75		[a]15.01
	3.0	517	5.54		13.66
		517	6.80		15.76
		690	7.39		16.31
		690	9.07		18.71

[a]Conditions for which maximum increase in penetration was found.

Helium Injection and Detection

The injection and measurement apparatus was essentially the same as that described in detail in reference 13. Ambient temperature helium was injected at total pressures of 331 to 897 kilonewtons per square meter through the injection nozzles into the supersonic crossflow. A small sampling probe (fig. 1) was mounted through the tunnel top wall on the centerline and located at nondimensional downstream positions x/d^* of 4.1, 10.1, 16.7, 17.2, and 17.8 where d^* is the nozzle throat diameter. Samples of the helium-air mixture were drawn into an on-line mass spectrometer at constant pressure and the resulting helium mole fraction output displayed on an x-y plotter. A complete set of test conditions and penetration results are given in table I.

RESULTS AND DISCUSSION

Concentration Measurements

Helium concentration measurements were made on a plane along the centerline of the flat plate directly downstream of the injection orifice. Typical centerplane concentration profiles are presented in figure 4 for some typical conditions studied. As the

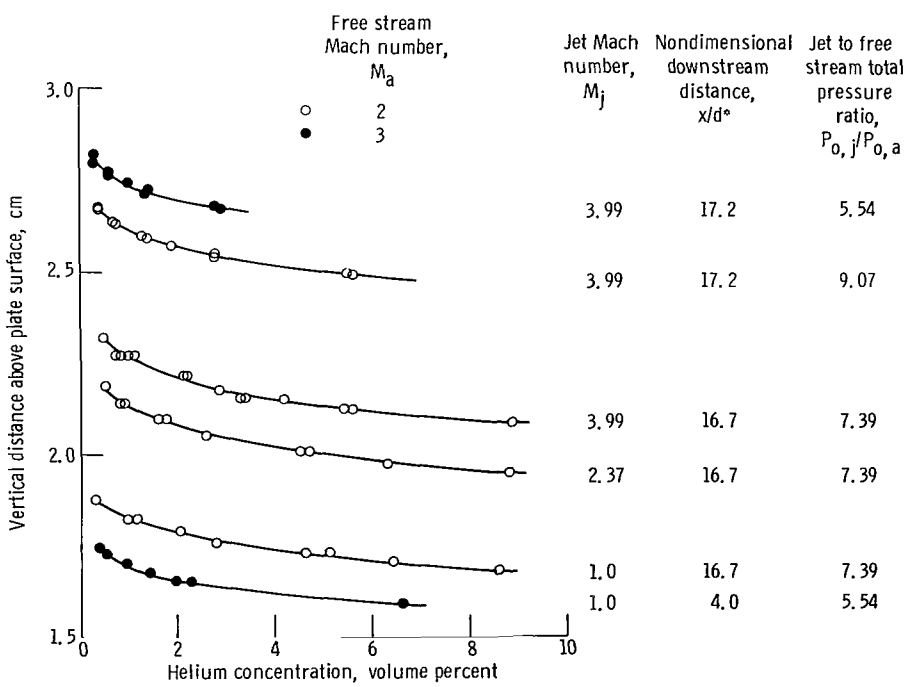

Figure 4. - Typical centerplane helium concentration data shown for various conditions.

probe was positioned farther from the plate surface, the measured helium concentration decreased until helium was no longer detected. As the probe was moved downstream, the profile shapes remained similar for the conditions tested. Complete profiles down to the plate surface were not obtained. The vertical distance at which a specific helium concentration was measured increased with increasing jet Mach number M_j, free stream Mach number M_a, downstream distance x/d^*, and increasing jet to free stream total pressure ratio $P_{o,j}/P_{o,a}$.

Since the absolute outer boundary of the jet (i.e., the point at which helium was no longer detected) was rather difficult to establish, a concentration of 0.5 percent by volume of helium was used as a definition of penetration. A similar definition has been used in references 1 to 3, 8, 10, and 14. In the subsequent discussion the position at which the 0.5 percent concentration was measured y' has been nondimensionalized by the nozzle throat diameter d^*; thus, all future mention of penetration means y'/d^*. Lateral rotations of the probe at y' verified that y' had a maximum value on the centerplane. Considering the errors in positioning the probe, measuring concentration, and fairing the curves (fig. 4), the estimated error in determining penetration was $\pm 0.125\ y'/d^*$ units.

Jet Mach Number Effect on Penetration

The effect of injection Mach number on penetration is shown in figure 5 for three downstream positions x/d^* of 4.1, 10.1, and 16.7 and total pressure ratios $P_{o,j}/P_{o,a}$ from 5.5 to 9.6. The free stream Mach number M_a was 2. Penetration increased with injection Mach number at each downstream position, with the effect of M_j on y/d^* increasing with x/d^*. At the first downstream station $x/d^* = 4.1$ (fig. 5(a)), a maximum increase of 13 percent occurred when M_j was increased from 1 to 4 at $P_{o,j}/P_{o,a} = 9.6$. Farther downstream (figs. 5(b) and (c)) more of an increase was observed, the maximum being about 25 percent at $x/d^* = 16.7$ and $P_{o,j}/P_{o,a} = 9.6$. The maximum increase found for all conditions studied (see footnoted values in table I) was about 30 percent. These comparisons were made between sonic and supersonic injection for cases of equal mass flow and equal jet total pressure. Straight lines were faired through the data in figure 5 for a later discussion of the correlation technique used.

Since the jet throat diameter was held fixed in this study, the jet exit pressure decreased with increasing jet Mach number for equal total pressure of the jet. Thus the jet was underexpanded at $M_j = 1$ and overexpanded at some higher Mach number. Although the data did not indicate any unusual behavior, the circular and square data points at $M_j = 3.99$ were those for which there may be a possibility of nozzle flow separation (see Model and Tunnel section).

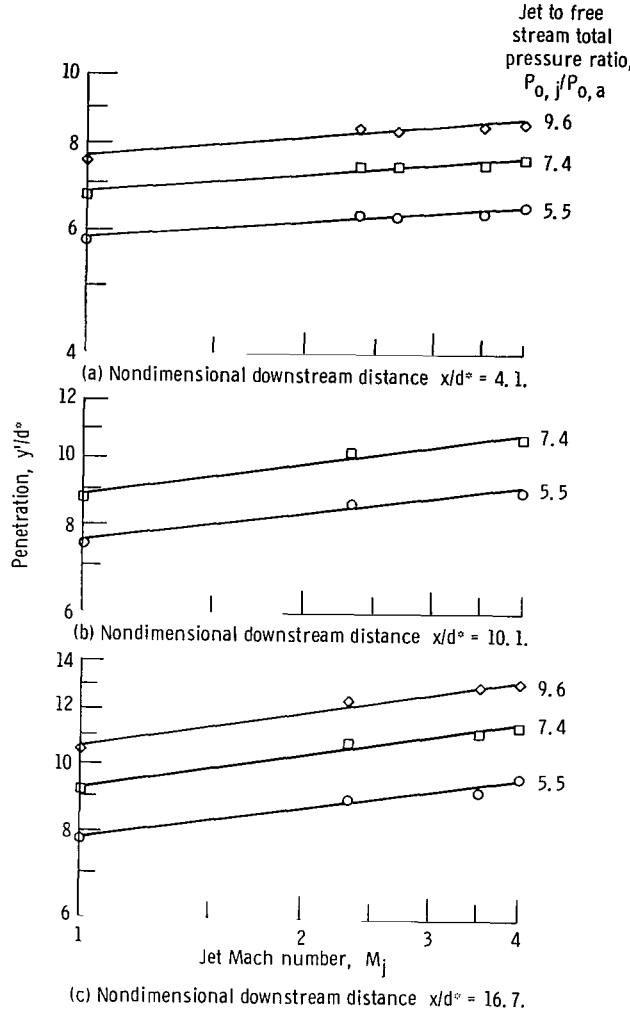

(a) Nondimensional downstream distance x/d* = 4.1.

(b) Nondimensional downstream distance x/d* = 10.1.

(c) Nondimensional downstream distance x/d* = 16.7.

Figure 5. - Variation of jet penetration with jet Mach number. (Free stream Mach number M_a = 2.)

Downstream Distance Effect on Penetration

Jet penetration increased with downstream distance as is shown in figure 6 for two different pressure ratios and for three jet Mach numbers. Most of the penetration occurred before the $x/d^* = 10.1$ position. The trajectory beyond this point flattened out and subsequent penetration probably occurred primarily because of turbulent mixing.

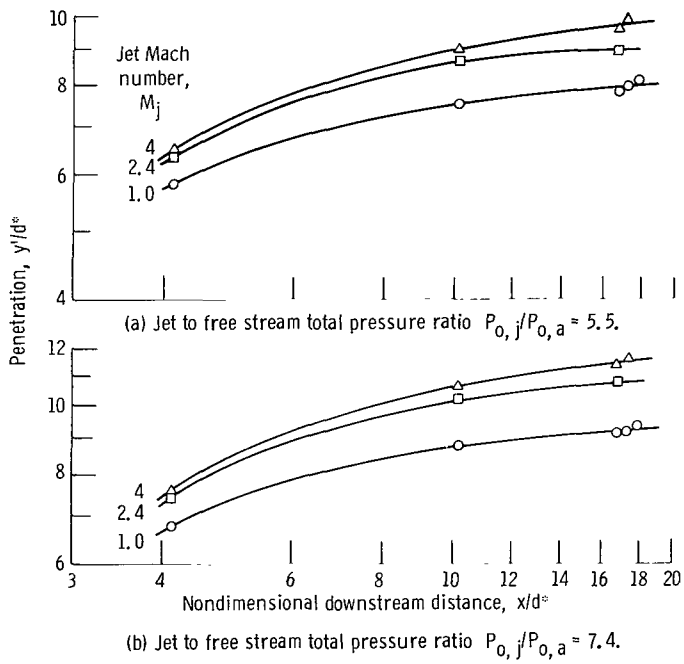

Figure 6. - Variation of jet penetration with downstream distance. (Free stream Mach number $M_a = 2.$)

Pressure Effects on Penetration

From figure 5 it was apparent that increasing the ratio of jet to free stream total pressure increased the jet penetration. The data reported in reference 12 showed that the penetration depended on this pressure ratio to approximately the one-half power. However, comparison of the top two curves of figure 4 shows that, as the free stream Mach number M_a was increased from 2 to 3, the penetration increased even though $P_{0,j}/P_{0,a}$ was reduced. The penetration at $M_a = 3$ was still proportional to $(P_{0,j}/P_{0,a})^{0.5}$ but a different penetration curve resulted for each free stream Mach number.

In order to determine the dependence of penetration on pressure for all pressure and Mach number conditions, a free stream effective back pressure P_{eb} was used as orig-

inally suggested in reference 5. This back pressure accounted for the complex shock and pressure field into which the jet was discharged and was defined in this study as two-thirds of the total pressure behind a normal shock in the free stream. This was the same definition used in references 8 and 15 and was within 5 percent of the back pressure based on static pressure mentioned previously and employed in references 6 and 11.

Data are plotted as a function of the jet total to effective back pressure ratio $P_{o,j}/P_{eb}$ in figure 7 where the open symbols denote $M_a = 2$ and the solid ones denote

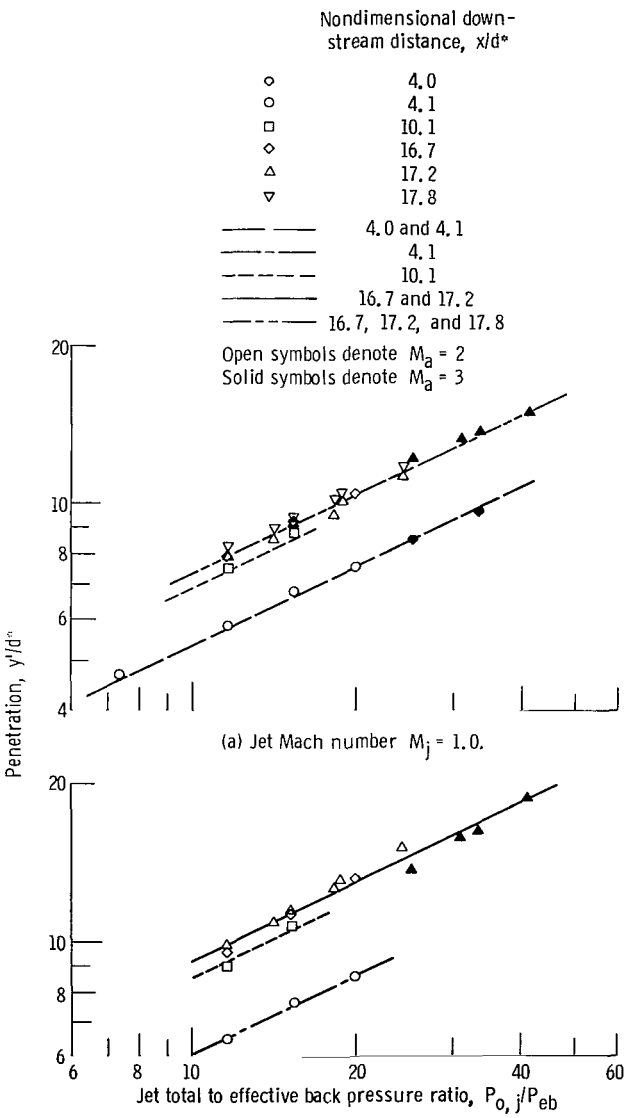

Figure 7. - Variation of penetration with pressure ratio; $y/d^* \propto (P_{o,j}/P_{eb})^{0.5}$.

$M_a = 3$. Two jet Mach numbers are shown and all downstream positions. Lines through the data were drawn with a slope of one-half to illustrate that penetration was still approximately dependent on pressure ratio to the 0.5 power. Data at a particular downstream distance all fall on the same line regardless of the free stream Mach number. Thus the effective back pressure concept was useful in correlating the effects on penetration of both tunnel total pressure changes and of pressure variations due to changes in free stream Mach number. The data for $x/d^* = 16.7$, 17.2, and 17.8 are shown (fig. 7) with a common line faired through them indicating little penetration variation over this x/d^* range.

If the penetration data are plotted as a function of momentum flux ratio $\rho_j v_j^2/\rho_a v_a^2$ as in references 1, 3, 8, and 12 rather than against pressure ratio, there still results a one-half power dependence as in the pressure ratio presentation. In this study, the pressure ratio has been chosen as a parameter with which to correlate the data since it was a directly controlled variable.

Correlation of Present Data

From the foregoing discussion it was shown that the jet penetration depended on jet Mach number, the downstream distance at which the measurements were made, the jet pressure, and some effective pressure in the free stream. Thus in order to correlate the data of this study, the following expression containing these variables was assumed:

$$\frac{y'}{d^*} = C\left(\frac{P_{o,j}}{P_{eb}}\right)^a (M_j)^b \left(\frac{x}{d^*} + 0.5\right)^c \tag{1}$$

where the constants C, a, b, and c are to be determined. The value of 0.5 in the last term results from the fact that the origin of the coordinate system is located at the center of the jet orifice whereas the upper jet boundary originates at the upstream edge of the orifice. Similar product-exponent-type correlation forms have been used in references 3, 11, 10, and 14; the latter two of which used dimensional analysis techniques to arrive at the correlation equation form. A multivariate regression analysis (ref. 16) was used to obtain those values of the constants C, a, b, and c which gave the best least-squares fit of the data. The resulting expression was

$$\frac{y'}{d^*} = 1.12\left(\frac{P_{o,j}}{P_{eb}}\right)^{0.483} (M_j)^{0.149} \left(\frac{x}{d^*} + 0.5\right)^{0.281} \tag{2}$$

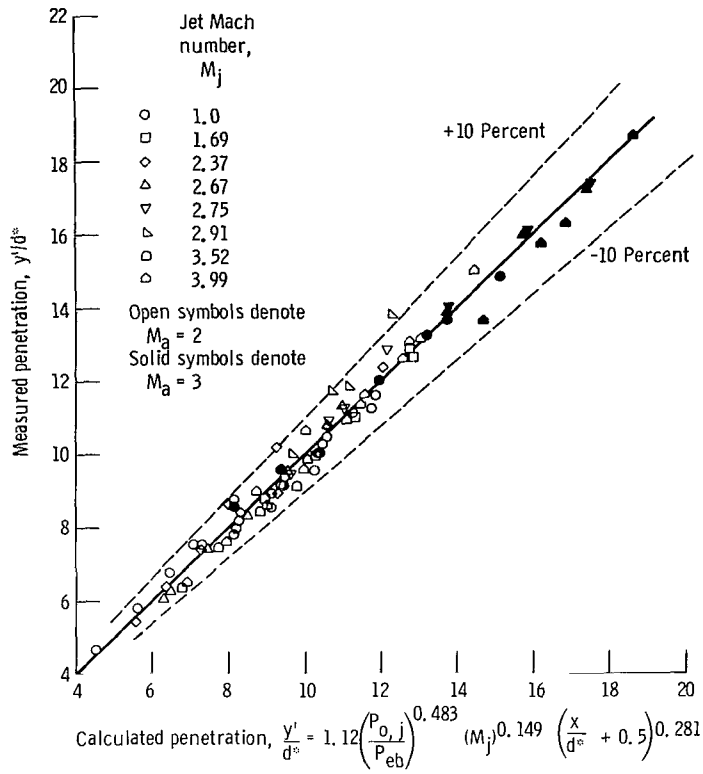

Figure 8. - Comparison of measured and calculated penetration for data of this study.

The measured penetration plotted against the penetration calculated from equation (2) is shown in figure 8 where the solid line is the line of equivalence between measured and calculated penetration. The agreement was within ±10 percent (represented by the dashed lines) for all but one data point. The limited data for expansion angles other than 17° are included and fall within the spread of the data. The trends with jet and free stream Mach number have been accounted for by the correlation equation.

The product-exponent form of correlation assumed in equation (1) and the subsequent linear regression analysis forced lines of constant slope through each of the independent variable plots (figs. 5 to 7). The straight lines faired through the data in figure 5 fit the data fairly well; however, the lines increase in slope with x/d^*. The analysis forced one best slope line (namely, $(y'/d^*) \propto (M_j)^{0.149}$ from eq. (2)) to fit all of these jet Mach number data. The dependence of penetration on x/d^* shown in figure 6 deviates from a constant slope relation. The correlation technique forced the best line with slope equal to 0.281 through the x/d^* data. The penetration dependence on pressure ratio was satisfactorily represented by a constant slope line of approximately 0.5 as shown in figure 7. The analysis yielded an exponent of 0.483 for $P_{o,j}/P_{eb}$. The Mach number and x/d^* terms could have been made to fit the data more realistically by using different equation

forms as was done in reference 12 where a hyperbolic form was used to improve the fit for the x/d^* data. However, in view of the correlation obtained simply with equation (2), the added complexity was not warranted.

Comparison with Other Work

The applicability of the correlation obtained for these data to other sets of data in the literature was tested. Data which used concentration measurements to determine penetration were chosen so the comparisons could all be made at the position of 0.5 percent concentration. Only one study was found (ref. 8) from which concentration measurements for supersonic injection could be obtained. Some studies (refs. 6 to 9 and 11) have used the Mach disk location (a shock feature of an underexpanded jet) as a measure of penetration. It was difficult to make a direct comparison between Mach disk location and outer boundary position, and so the Mach disk data of these studies were not included. The following is a brief description of the studies used for comparison; all employed injection normal to the free stream from a flat plate.

In reference 2 Torrence injected various molecular weight gases at sonic velocity into a Mach 4.03 stream having a thick boundary layer. Only the data for hydrogen and helium were chosen for comparison since Torrence showed an effect of molecular weight on penetration especially for heavier gases. In the same wind tunnel used by Torrence, Rogers (ref. 3) studied the effect of the momentum of sonically injected hydrogen on jet penetration. In reference 8, Orth and Funk determined hydrogen penetration by Mach disk position and by concentration measurements for sonic and supersonic injection into a Mach 2.72 airstream. Supersonic injection Mach numbers of 1.31, 1.50, and 1.73 were used. Some additional unpublished injection studies were made at the Lewis Research Center by L. Povinelli and R. Ehlers in a 12.7- by 6.35-centimeter Mach 2.7 wind tunnel. Helium total injection pressure was varied from 435 to 1455 kilonewtons per square meter, while tunnel pressure varied from 274 to 1033 kilonewtons per square meter. Concentration measurements were made at $x/d^* = 5.4$.

The penetration data from these four studies have been compared to the penetration calculated from equation (2). The correlation underpredicted the penetration in all cases. A least-squares line through the data of reference 8 was within about one jet diameter of the present data; the least-squares lines of references 2 and 3 were underpredicted by about two jet diameters; and the unpublished NASA penetration data were underpredicted by about one to four jet diameters. Thus equation (2) is not widely applicable but applies only to the set of data obtained under the conditions of the present study. When the data of all five studies were subjected simultaneously to the regression analysis with equation (1) as the correlation form, a considerably better correlation resulted but one which was still unsatisfactory.

One parameter which has not been taken into consideration in this comparison and which was significantly different between the experiments was the boundary layer thickness. Schetz and Billig (ref. 5) have introduced the boundary layer thickness as a possible controlling parameter in the penetration of underexpanded jets. A thick boundary layer would shield the injected jet from the high momentum free stream for a greater distance than would a thin boundary layer. Rogers in reference 3 has suggested the different boundary layer thicknesses as a possible reason for disagreement between his data and previous correlations in the literature. Since the boundary layer thicknesses were so widely varied in the experiments considered here, this variation was explored as a possible reason for the poor agreement when all of the data were compared to equation (2).

Torrence measured the turbulent boundary layer thickness to be three times the jet diameter ($\delta/d^* = 3$). Similarly, Rogers measured a δ/d^* of 2.7 in the same tunnel. A value of approximately 0.2 was reported in reference 17 for the data of Orth and Funk. The laminar boundary layer thickness for the present study was estimated from $\delta = 5.5\ell/Re_L^{0.5}$ (ref. 18), and the turbulent thickness for the NASA unpublished data was estimated from $\delta = 0.37\ell/Re_L^{0.2}$ (ref. 19). These estimates resulted in δ/d^* values ranging from 0.214 to 0.319 and 0.871 to 1.11, respectively, for the two studies. Free stream momentum is lost due to viscous shear in the boundary layer; since penetration depends on the free stream momentum, the momentum thickness θ rather than the velocity thickness δ was used as the boundary layer correction term. Values of θ/d^* were calculated from tabulated θ/δ values given in reference 20, using a velocity profile exponent of 1/5 for the laminar data and 1/7 for the turbulent data. Table II presents the nondimensionalized boundary layer velocity thickness and momentum thickness for the studies being compared.

TABLE II. - NONDIMENSIONALIZED BOUNDARY LAYER VELOCITY THICKNESS AND MOMENTUM THICKNESS FOR VARIOUS STUDIES

Source	Nondimensional velocity thickness, δ/d^*	Nondimensional momentum thickness, θ/d^*
Present data	0.214 to 0.319	0.020 to 0.025
Ref. 2	3	0.157
Ref. 3	2.7	0.141
Ref. 8	0.2	0.0165
Unpublished NASA data	0.878 to 1.11	0.062 to 0.079

The nondimensionalized momentum thickness term θ/d^* was included in the following correlation expression in the form:

$$\frac{y'}{d^*} = C\left(\frac{P_{o,j}}{P_{eb}}\right)^a (M_j)^b \left(\frac{x}{d^*} + 0.5\right)^c \left(\frac{\theta}{d^*}\right)^d \tag{3}$$

where d was another constant to be determined in the regression analysis. All five sets of data were included with the result being

$$\frac{y'}{d^*} = 3.21\left(\frac{P_{o,j}}{P_{eb}}\right)^{0.416} (M_j)^{0.121} \left(\frac{x}{d^*} + 0.5\right)^{0.203} \left(\frac{\theta}{d^*}\right)^{0.163} \tag{4}$$

The measured penetrations are plotted as a function of the penetration calculated from equation (4) in figure 9. The solid line is a line of equivalence between measured and calculated penetration and the dashed lines are ±15 percent variation about the line of equivalence. The key in figure 9 gives the ranges of variables for each of the studies. Upon comparison of equations (2) and (4), it is seen that not only was a momentum thickness correction term added but also an alteration in the constants resulted in order to fit all sets of data. The approximately half-power penetration dependence on pressure ratio changed to $(P_{o,j}/P_{eb})^{0.416}$ and the exponents of M_j and x/d^* decreased somewhat. Thus, even though the penetration dependence on each independent variable noted in equation (4) may not be exactly correct, the simple equation form does correlate (to within ±15 percent) a large amount of data taken in different tunnels over widely varying conditions.

In an attempt to improve this correlation and recognizing that most of the jet penetration occurred near the injection location, the data were divided into near field ($x/d^* \leq 7$) and far field ($x/d^* > 7$) regions. This x/d^* break point was somewhat arbitrary but was based on results given in references 3, 8, 15, and 17 which indicated a change in penetration behavior at $7 \leq x/d^* \leq 10$, and also on the fact that the data available were conveniently separated at this point. In the far field, all data points but two agreed to within ±10 percent of that calculated by

$$\frac{y'}{d^*} = 2.96\left(\frac{P_{o,j}}{P_{eb}}\right)^{0.405} (M_j)^{0.163} \left(\frac{x}{d^*} + 0.5\right)^{0.204} \left(\frac{\theta}{d^*}\right)^{0.141} \tag{5}$$

The near field correlation resulted in little improvement over that obtained with equation (4).

Source	Jet Mach number, M_j	Jet total to effective back pressure ratio, $P_{o,j}/P_{eb}$	Nondimensional downstream distance, x/d^*	Free stream Mach number, M_a
○ Present results	1 to 4	7.4 to 41	4 to 18	2 to 3
□ Ref. 8	1 to 1.7	2.8 to 5.2	1.7 to 11	2.72
◇ Ref. 3	1	1.1 to 3.2	7 to 200	4.03
△ Ref. 2	1	2 to 2.2	7 to 200	4.03
⌂ Unpublished NASA data	1	1.5 to 19	5.4	2.7

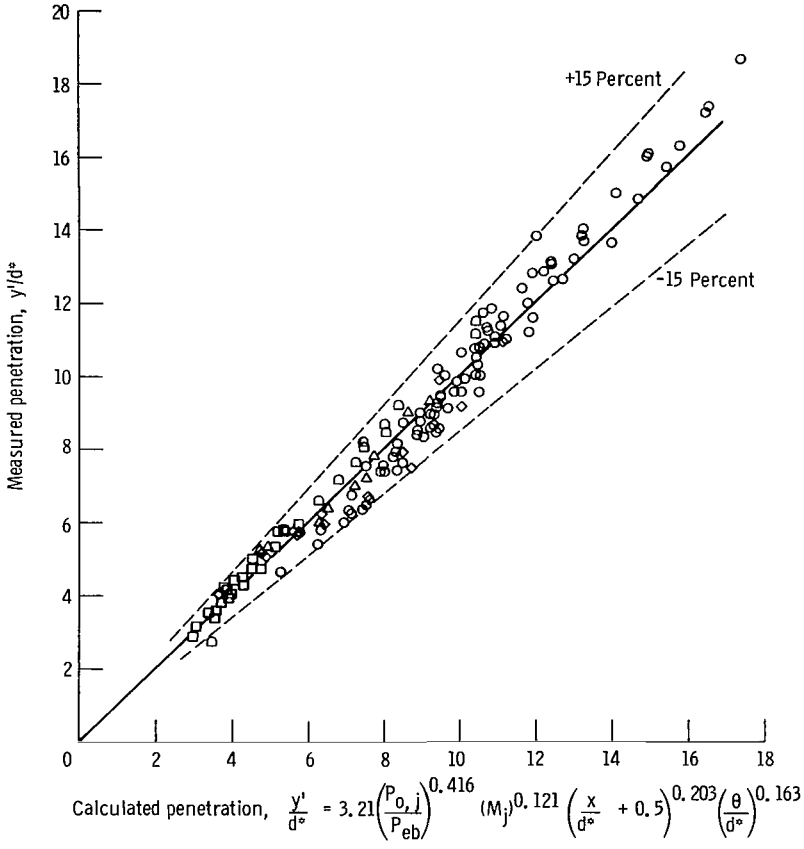

Figure 9. - Comparison of measured and calculated penetration for all sets of data with boundary layer momentum included in correlation.

SUMMARY OF RESULTS

Helium was injected at various Mach numbers ranging from 1 to 4 into supersonic crossflows at Mach 2 and 3. Concentration measurements were taken downstream and the penetration of the helium jets was characterized by the 0.5 mole fraction boundary. The significant results are summarized as follows:

1. Penetration increased with injection Mach number when mass flows and total pressures were held constant. The effect of injection Mach number on penetration increased

with downstream distance. A maximum increase of approximately 30 percent in penetration was found for Mach 4 injection over sonic injection.

2. Penetration increased with downstream distance. Most of the penetration was obtained close to the injection orifice at nondimensionalized distances of ten or less.

3. Jet penetration was proportional to the jet total to effective back pressure ratio raised to the one-half power. Effective back pressure correlated penetration data for changes in tunnel total pressure and Mach number.

4. Penetration data from this study were correlated with an expression containing the jet total to effective back pressure ratio, jet Mach number, and downstream distance. The data agreed with the correlation equation to within ±10 percent. The equation did not correlate data from other studies found in the literature because the boundary layer thickness was not considered.

5. Addition of a boundary layer momentum thickness to the equation correlated the data from four other jet penetration studies. Agreement to within ±15 percent was obtained. Separating the data into near field and far field regions improved the correlation in the far field.

Lewis Research Center,
National Aeronautics and Space Administration,
Cleveland, Ohio, March 16, 1971,
722-03.

REFERENCES

1. Torrence, Marvin G.: Concentration Measurements of an Injected Gas in a Supersonic Stream. NASA TN D-3860, 1967.

2. Torrence, Marvin G.: Effect of Injectant Molecular Weight on Mixing of a Normal Jet in a Mach 4 Airstream. NASA TN D-6061, 1971.

3. Rogers, R. Clayton: A Study of the Mixing of Hydrogen Injected Normal to a Supersonic Airstream. NASA TN D-6114, 1971.

4. Zukoski, Edward E.; and Spaid, Frank W.: Secondary Injection of Gases into a Supersonic Flow. AIAA J., vol. 2, no. 10, Oct. 1964, pp. 1689-1696.

5. Schetz, Joseph A.; and Billig, Frederick S.: Penetration of Gaseous Jets Injected into a Supersonic Stream. J. Spacecraft Rockets, vol. 3, no. 11, Nov. 1966, pp. 1658-1665.

6. Schetz, Joseph A.; Hawkins, Paul F.; and Lehman, Harry: Structure of Highly Underexpanded Transverse Jets in a Supersonic Stream. AIAA J., vol. 5, no. 5, May 1967, pp. 882-884.

7. Chrans, Larry J.; and Collins, Daniel J.: Stagnation Temperature and Molecular Weight Effects in Jet Penetration. AIAA J., vol. 8, no. 2, Feb. 1970, pp. 287-293.

8. Orth, Richard C.; and Funk, John A.: An Experimental and Comparative Study of Jet Penetration in Supersonic Flow. J. Spacecraft Rockets, vol. 4, no. 9, Sept. 1967, pp. 1236-1242.

9. Koch, Larry N.; and Collins, Daniel J.: The Effect of Varying Secondary Mach Number and Injection Angle on Secondary Gaseous Injection into a Supersonic Flow. Paper 70-552, AIAA, May 1970.

10. Vranos, A.; and Nolan, J. J.: Supersonic Mixing of a Light Gas and Air. Presented at the AIAA Propulsion Joint Specialist Conference, Colorado Springs, Colo., June 14-18, 1965.

11. Schetz, Joseph A.; Weinraub, Robert A.; and Mahaffey, Raymond E., Jr.: Supersonic Transverse Injection into a Supersonic Stream. AIAA J., vol. 6, no. 5, May 1968, pp. 933-934.

12. Povinelli, Frederick P.; Povinelli, Louis A.; and Hersch, Martin: Supersonic Jet Penetration (up to Mach 4) into a Mach 2 Airstream. J. Spacecraft Rockets, vol. 7, no. 8, Aug. 1970, pp. 988-992.

13. Povinelli, Frederick P.; Povinelli, Louis A.; and Hersch, Martin: Effect of Angle of Attack and Injection Pressure on Jet Penetration and Spreading from a Delta Wing in Supersonic Flow. NASA TM X-1889, 1969.

14. Faucher, Joseph F., Jr.; Goldstein, Sidney; Seery, Daniel J.; and Taback, Edward: Supersonic Combustion of Fuels Other than Hydrogen for Scramjet Applications. Rep. E910358-23, United Aircraft Corp. (AFAPL-TR-67-12, DDC No. AD-379427L), Feb. 1967.

15. Billig, F. S.; Orth, R. C.; and Lasky, M.: A Unified Approach to the Problem of Gaseous Jet Penetration into a Supersonic Stream. Paper 70-93, AIAA, Jan. 1970.

16. Sidik, Steven M.; and Henry, Bert: Rapier - A FORTRAN IV Program for Multiple Linear Regression Analysis Providing Internally Evaluated Remodeling. NASA TN D-5656, 1970.

17. Henry, John R.: Recent Research on Fuel Injection and Mixing and Piloted - Ignition for Scramjet Combustors. Twelfth Symposium (International) on Combustion. Combustion Institute, 1969, pp. 1175-1182.

18. Howarth, L., ed.: Modern Developments in Fluid Dynamics. Vol. I. Clarendon Press, Oxford, 1953.

19. Schlichting, Hermann (J. Kestin, trans.): Boundary Layer Theory. McGraw-Hill Book Co., Inc., 1955.

20. Persh, Jerome; and Lee, Roland: Tabulation of Compressible Turbulent Boundary Layer Parameters. NAVORD Rep. 4282, Aeroballistics Res. Rep. 337, Naval Ordnance Lab., May 1, 1956.

15U 001 26 51 3DS 71166 00903
AIR FORCE WEAPONS LABORATORY /WLOL/
KIRTLAND AFB, NEW MEXICO 87117

ATT E. LOU BOWMAN, CHIEF,TECH. LIBRARY

"The aeronautical and space activities of the United States shall be conducted so as to contribute . . . to the expansion of human knowledge of phenomena in the atmosphere and space. The Administration shall provide for the widest practicable and appropriate dissemination of information concerning its activities and the results thereof."

— NATIONAL AERONAUTICS AND SPACE ACT OF 1958

NASA SCIENTIFIC AND TECHNICAL PUBLICATIONS

TECHNICAL REPORTS: Scientific and technical information considered important, complete, and a lasting contribution to existing knowledge.

TECHNICAL NOTES: Information less broad in scope but nevertheless of importance as a contribution to existing knowledge.

TECHNICAL MEMORANDUMS: Information receiving limited distribution because of preliminary data, security classification, or other reasons.

CONTRACTOR REPORTS: Scientific and technical information generated under a NASA contract or grant and considered an important contribution to existing knowledge.

TECHNICAL TRANSLATIONS: Information published in a foreign language considered to merit NASA distribution in English.

SPECIAL PUBLICATIONS: Information derived from or of value to NASA activities. Publications include conference proceedings, monographs, data compilations, handbooks, sourcebooks, and special bibliographies.

TECHNOLOGY UTILIZATION PUBLICATIONS: Information on technology used by NASA that may be of particular interest in commercial and other non-aerospace applications. Publications include Tech Briefs, Technology Utilization Reports and Technology Surveys.

Details on the availability of these publications may be obtained from:

SCIENTIFIC AND TECHNICAL INFORMATION OFFICE

NATIONAL AERONAUTICS AND SPACE ADMINISTRATION

Washington, D.C. 20546